

MONTE-CARLO AND POLYHEDRON-BASED SIMULATIONS I:  
EXTREMAL STATES OF THE LOGARITHMIC N-BODY  
PROBLEM ON A SPHERE

CHJAN C. LIM, JOSEPH NEBUS, AND SYED M. ASSAD

*Dedicated to Professor Lawrence Sirovich on the occasion of his 70th birthday.*

(Communicated by Ka-Kit Tung)

ABSTRACT. The problem of  $N$  bodies on the surface of the sphere interacting by a logarithmic potential is examined for selected  $N$  ranging from 4 to 40,962, comparing the energies found by placing points at the vertices of certain polyhedrons to the lowest energies found by a Monte Carlo algorithm. The polyhedron families are generated from simple polyhedrons through two triangular face splitting operations which are used iteratively to increase the number of vertices. The closest energy of these polyhedron vertex configurations to the Monte Carlo-generated minimum energy is identified and the two energies are found to agree well. Finally the energy per particle pair is found to asymptotically approach a mean field theory limit of  $-\frac{1}{2}(\log(2) - 1)$ , approximately 0.153426, for both the polyhedron and the Monte Carlo-generated energies. The deterministic algorithm of generating polyhedrons is shown to be a method able to generate consistently good approximations to the extremal energy configuration for a wide range of numbers of points.

**1. Introduction.** Consider  $N$  point vortices, all of uniform strength, on the surface of the unit sphere. If the positions of these vortices are given by  $\vec{x}_1, \vec{x}_2, \dots, \vec{x}_N$  then the energy of this system is [7] [10] [12] [13]

$$E = - \sum_{1 \leq j < k \leq N} \log|1 - \vec{x}_j \cdot \vec{x}_k| \quad (1)$$

(with possibly a constant multiplying the sum). Extremal configurations of these points are of great interest. It has been seen [11] that a Monte Carlo-based algorithm is able to find numerically configurations which are local minimums of the potential energy function [2]. One may also approach energy minimums by algorithmic approaches which try to uniformly place points over the surface of the sphere [3] [13]. This problem is equivalent to that of maximizing the product of distances between points, but related problems include that of spherical codes which try to maximize the minimum distance between points, or the Thompson problem of equal electrical charges on the sphere [1] [4]. These related problems yield similar but not identical results.

In this paper an approach based on solid geometries is considered. A set of points on the surface of the sphere appears naturally to correspond to the vertices of certain polyhedrons (for example, four vortices of uniform strength will on the

---

<sup>1</sup>Corresponding author: [limc@rpi.edu](mailto:limc@rpi.edu). Mathematics Department, Rensselaer Polytechnic Institute, Troy, NY 12180 USA.

sphere reach an energy minimum at the vertices of a tetrahedron). This leads to the approach of constructing polyhedrons and using the locations of the vertices of those as points on which to place vortices on the sphere. One begins with a base polyhedron, in this paper one with exclusively triangular faces, and constructs more complex polyhedrons from that shape. With these generated polyhedrons then one places vortices of uniform strength at each vertex and studies the Hamiltonian of that configuration.

Obviously not all polyhedrons may be used in this approach. Only polyhedrons which can have all vertices fit on the surface of the sphere are applicable. The set of base polyhedrons used for this paper (section 4) begins with several which do fit the surface of the sphere (and whose vertices furthermore correspond to an energy minimum for vortices). To construct a more complex polyhedron one applies one of the ‘face splitting’ operations.

Either of the face splitting operations used in this paper (sections 4.1 and 4.2) takes an existing triangular face and adds one or more vertices to the portion of the sphere’s surface radially outward from that face. New edges are then drawn from the original face’s vertices to the new vertices added by the operation, and new faces are drawn among the original and added points. This construction splits the original triangular face into multiple new triangular faces, and increases the number of vertices in the polyhedron, but still creates a polyhedron with its vertices on the surface of the sphere and which may then be split again.

Only two face splitting operations are considered as they yielded a large enough set of shapes to be interesting, but there is no reason to suppose there are not more operations which could be employed by similar techniques. Saaf and Kuiljaars, studying spherical coding, outline a ‘spiral placing’ of points which appears fittable to the faces here [13]. The lattices explored by Bowick, Cacciuto, Nelson, and Travesset [4] and the triangulations used by Altschuler, Williams, Ratner, Tipton, Stong, Dowla, and Wooten [1] and those used by Baumgardner and Frederickson [3] also suggest face splitting operations which could be productive for this sort of polyhedron-based investigation.

Also in this paper only a single face splitting operation was done at each iteration, with the same split performed for every face of the old polyhedron. Extensions to this routine to split different faces by different rules can be imagined, but are not as obviously organized for convenient study.

The original shapes enjoy a nearly uniform vertex degree count, with most vertices being as connected as any other vertex is. It is found applying these face splitting operations may disrupt the uniformity of the vertex degrees, but argued that the vertex degrees are not of interest in this problem – the edges are an artifact of the polyhedrons used to place points and are not of physical meaning (section 4.4). The edges may be redrawn for convenience.

As a result by repeatedly applying a choice of the face splitting operations one can create a binary tree-like structure of polyhedrons of increasing degree (section 4.3). As the two face splitting operations considered here do not commute the placement of points, but do generate the same number of points whichever order they are applied in (section 4.5), the binary tree-like structure is more compelling (section 4.6). One can create several distinct polyhedrons with equal numbers of vertices and still different energies (section 5).

The vertices of certain generated polyhedrons are found to have energies close to the extremal state energy as generated by a Monte Carlo algorithm (sections 2,

5). The polyhedrons generated from the tetrahedron (section 6), from the octahedron (section 7), and the icosahedron (section 8) are examined, to locate minimum energies generated by the Monte Carlo method for an equal number of vortices.

The energy per particle pair is compared for the vortices placed at the polyhedron configurations as well as for the Monte Carlo-generated extremal states, and it is found both pairwise energies agree with one another (section 9.1) and tend, in the limit as the number of particles grows infinitely large, asymptotically towards a mean field limit [2] (section 9.2) (cf Lim [9]) which is found to be a pairwise particle energy of approximately 0.153426.

## 2. Numerical Tools.

**2.1. Monte Carlo Algorithm.** Given a system of  $n$  point vortices, all of uniform strength (assumed to be 1), the potential energy will be

$$H(\vec{z}_1, \vec{z}_2, \dots, \vec{z}_n) = - \sum_{1 \leq j < k \leq n}^n \log |1 - \vec{z}_j \cdot \vec{z}_k| \quad (2)$$

for particles on the surface of the sphere (with  $\vec{z}_j = (x_j, y_j, z_k)$  the coordinates of vortex  $j$ , and the constraint that  $|\vec{z}_j| \equiv 1$  for all  $j$ ) [7] [8] [12].

A Metropolis-rule Monte Carlo algorithm is employed to find an equilibrium configuration for this system. Each sweep is a series of  $n$  experiments, in each of which one vortex is (randomly) selected. On each vortex a proposed displacement is tested: Consider moving the chosen vortex by a rotation around a randomly selected axis by an angle uniformly distributed on  $(0, \epsilon)$ . The change in energy  $\Delta H$  this rotation would cause is calculated. Based on a preselected inverse temperature  $\beta$ , and a randomly chosen number  $r$  uniformly distributed on  $(0, 1)$ , the change is

$$\left\{ \begin{array}{l} \text{accepted if } r < \exp -\beta\Delta H \\ \text{rejected if } r \geq \exp -\beta\Delta H \end{array} \right\}$$

This is the Metropolis Rule for Monte Carlo algorithms. (Note that if  $\beta$  is positive this results in any change which decreases energy being accepted. A negative inverse temperature  $\beta$ , while not theoretically objectionable for this problem, is uninteresting – it results in the vortices clustering together, rather than to spreading out over the physical domain.)

This process of consideration and acceptance or rejection is repeated for each of the  $n$  experiments in the sweep. The sweeps are repeated until either a statistical equilibrium is achieved or a preselected number of sweeps has been allowed to elapse. In this paper waiting for a preselected number of sweeps to complete is used.

The use of just a finite number of sweeps before considering the system to be at or nearly at the energy minimum is justified by figure 1, in which the energy of the system (per number of pairs of particles) is compared for a variety of numbers of vortices. In each case the energy (per pair) declines rapidly from an initial value and settles to a nearly uniform level within several hundred sweeps. For up to 642 vortices just 500 sweeps suffices to reach this extremal configuration.

It is an unavoidable consequence of the Monte Carlo algorithm that it is unlikely to produce exactly the global minimum for any number of points. Suppose that one particle is out of this ‘exact’ position by a small angle. The likelihood that a Monte Carlo sweep, when it does pick this vortex to move, will pick just the correct direction and just the correct angle to fit the vortex exactly in place is tiny. However,

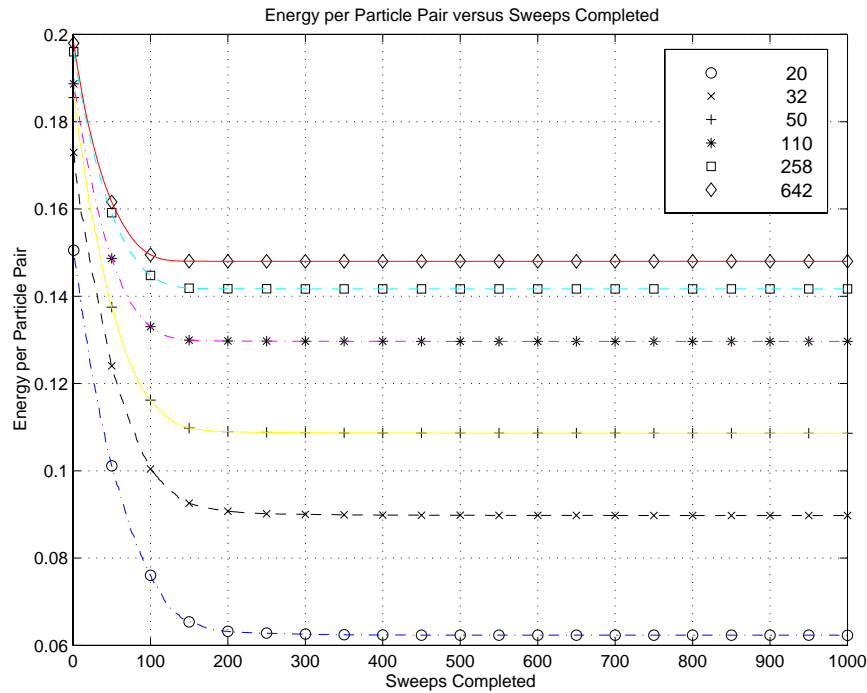


FIGURE 1. System energy (per pair of points) versus the number of sweeps completed for 20, 32, 50, 110, 258, and 642 points on the surface of the sphere. Convergence occurs within several hundred sweeps, as it appears to do for the range of  $N$  values examined in this paper.

the difficulty in these exact matches is caused by the system reaching a very good configuration within these first several hundred sweeps – the moves which produce great decreases in the system energy are made, and only incremental improvements remain available.

It is also a consequence that as the Monte Carlo algorithm produces a statistical equilibrium it is not guaranteed that the points generated are near a dynamic equilibrium. If each attempted move of a point may spread over a wide enough region, and the inverse temperature used to drive the system toward equilibrium is large enough, it is likely that local minimums will be escaped.

Nevertheless these problems do persist with the Monte Carlo algorithm, and result in a handful of anomalies such as that seen in sections 8.3.1 and 8.3.2, in which the Monte Carlo algorithm does not (in its 40,000 sweeps) reach an energy quite as low as that achieved by the icosahedron split by the geodesic word  $CG$  (section 4).

**2.2. Radial Distribution Function.** The radial distribution function – a term which is borrowed from the statistical mechanics of gases – studies the density of particles relative to a uniform density, at a given radius from any given reference point [6]. In this paper the use of such a function is straightforward – the vortex

particles behave in some ways like a gas – and so it serves as a tool by which the structure of the system can be measured (cf. also Lim, Nebus, and Assad [11]).

The radial distribution function is defined for a given angular separation  $\theta$ . (This separation is equivalent, on the surface of the unit sphere, to the distance  $\theta$ .) It is constructed here to be the set of ordered pairs of angular separations  $\theta$  with the number of pairs which have that separation.

**Definition 1.** For a set of particles  $\vec{x}_j, j = 1 \dots N$  define the radial distribution function to be the set of ordered pairs

$$D = \{(\theta, n) \mid n \text{ is the number of pairs of points with separation } \theta\} \tag{3}$$

– that is,  $\theta$  is a radial separation with  $n$  pairs of points with that separation.

In the studies of gas and crystal properties from which the notion of a radial distribution function is derived, the radial distribution function is taken to be the number of pairs separated by a given range of distances, divided by the number of pairs which would be expected in a completely uniform distribution – typically meaning one divides the number of particles in a shell by a uniform density times the volume of that shell [6]. For this paper that normalization is not used.

In this paper graphs of the radial distribution functions are simplified by grouping together angles which are  $\Delta\theta = \frac{\pi}{180}$  apart, making the plots represent the numbers of vertices per degree apart.

**3. The Mean Field Limit.** The problem of point vortices on the sphere is believed to take on a mean field limit as the number of particles grows infinitely large (cf Bergersen’s calculations in [2]). One can estimate the expected energy per particle pair for this continuum limit because as the number of particles grows infinitely large the most probable vorticity distribution becomes a uniform density  $\rho$ . Then one calculates the expected total energy to be

$$E = -\frac{1}{2} \int_D \int_{D'} \rho^2 \log |1 - \vec{x} \cdot \vec{y}| dA dA'$$

where  $D$  is the surface of the unit sphere,  $dA$  is at  $\vec{x}$  and  $dA'$  is at  $\vec{y}$ . The factor  $\frac{1}{2}$  was introduced to prevent double counting of each particle pair. If one first keep  $\vec{x}$  at  $\theta = 0$  and perform the integration over  $dA'$ , one has

$$\begin{aligned} E &= -\frac{1}{2} \int_D \int_{D'} \rho^2 \log |1 - \cos(\theta')| dA dA' \\ &= -\frac{1}{2} \rho^2 \int_D dA \int_0^{2\pi} d\phi' \int_0^\pi d\theta' \log |1 - \cos \theta'| \sin \theta' \\ &= -\frac{1}{2} \rho^2 \int_D dA 2\pi (2 \log 2 - 2) \end{aligned} \tag{4}$$

Now if one integrates over  $dA$ , one would get

$$E = -\frac{1}{2} \rho^2 8\pi^2 (2 \log 2 - 2)$$

For sufficiently large finite values of  $N$ , by setting the vortex density  $\rho = \frac{N}{4\pi}$  in equation 4, one obtains the following bounds for the expected total energy  $E_N$

$$0 \leq E_N \leq -\frac{1}{2} \frac{N^2}{2} (2 \log 2 - 2)$$

with  $E_N$  the most probable energy for this uniformly spread point particles.

But more than that, the mean field limit (if it holds) states that

$$\lim_{N \rightarrow \infty} \frac{E_N}{N^2} = -\frac{1}{2}(\log 2 - 1) \sim 0.153426$$

Thus as the number of vortices grows, the mean field energy per particle pair will approach a constant of approximately 0.153426. The numerical results examined in section 9.2 and plotted in figures 9 and 10 strongly support the existence of this mean field limit in this problem.

**4. Polyhedron Shapes.** Begin with a convex polyhedron with faces composed entirely of triangles. Though the faces need not be regular, the Platonic solids of the tetrahedron, the octahedron, and the icosahedron form a useful basic set and (as is seen in sections 6.1, 7.1, and 8.1) all represent extremal states for the vortex problem with the corresponding number of vortices.

Daud Sutton considers [14] many polyhedron shapes which may be constructed by performing several operations on polyhedra of fewer vertices. Such operations include the taking of duals to existing polyhedra, truncating the vertices of a shape, compounding of several polyhedra together, twisting of edges, and the like. This opens a great array of shapes to consider. For this paper, a minimal set of operations – called the centroid split and the geodesic split – are used to construct robust families of polyhedra.

#### 4.1. Centroid Splitting.

**Definition 2.** *The Centroid split of a triangle  $ABC$  is to add to it a point  $D$  where the ray beginning at the center of the sphere and passing through the centroid of  $ABC$  intersects the sphere, and adding to the polyhedron the edges  $AD$ ,  $BD$ , and  $CD$ .*

This construction does not preserve the degrees of the original points  $A$ ,  $B$ , or  $C$ , but it is argued in section 4.4 such degree counts are arbitrary properties and do not require any attention.

This splitting increases the number of vertices in the polyhedron by the number of faces, triples the number of faces, and adds three times the number of faces to the number of edges. From this construction the count of vertices, edges, and faces in the new polyhedron is:

$$\begin{aligned} v' &= v + f \\ e' &= e + 3f \\ f' &= 3f, \end{aligned} \tag{5}$$

An apparent anomaly of the centroid splitting is that certain configurations may appear to create a square face from what was originally a polyhedron with only triangular faces – notably, if one takes the centroid split of a regular tetrahedron the result has vertices at the corners of the cube. If one does not lose the edge information as originally created this effect will not propagate – either the geodesic or the centroid split after this shape will restore the figure to what are clearly triangular faces.

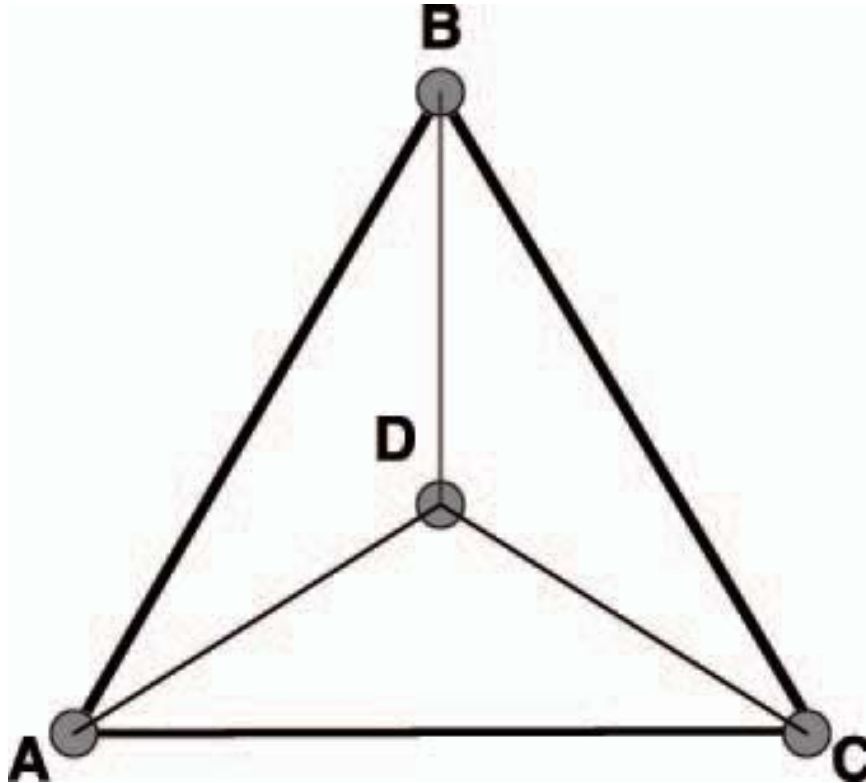


FIGURE 2. An example of the centroid split. The centroid of the planar triangle  $ABC$  is added, and then the point at which the ray from the center of the sphere passing through this centroid is added as  $D$ . The edges  $AD$ ,  $BD$ , and  $CD$  are added.

#### 4.2. Geodesic Splitting.

**Definition 3.** *The Geodesic split of a triangle  $ABC$  is to add to it a point  $E$  where the ray from the center of the sphere and passing through the midpoint of  $AB$  intersects the sphere, a point  $F$  similarly based on the bisection of  $BC$ , and a point  $G$  similarly based on the bisection of  $CA$ , and adding to the polyhedron the edges  $EF$ ,  $FG$ , and  $GE$ , and furthermore adding edges  $AE$  and  $EB$  in place of  $AB$ , adding edges  $BF$  and  $FC$  in place of  $BC$ , and edges  $CG$  and  $GA$  in place of  $CA$ .*

This splitting preserves the degrees of the original polyhedron's vertices, and adds only vertices of degree six.

This splitting increases the number of vertices in the polyhedron by the number of edges, quadruples the number of faces, and doubles and then adds three times the number of faces to the number of edges. From this construction the count of vertices, edges, and faces in the new polyhedron is:

$$\begin{aligned} v' &= v + e \\ e' &= 2e + 3f \\ f' &= 4f, \end{aligned} \tag{6}$$

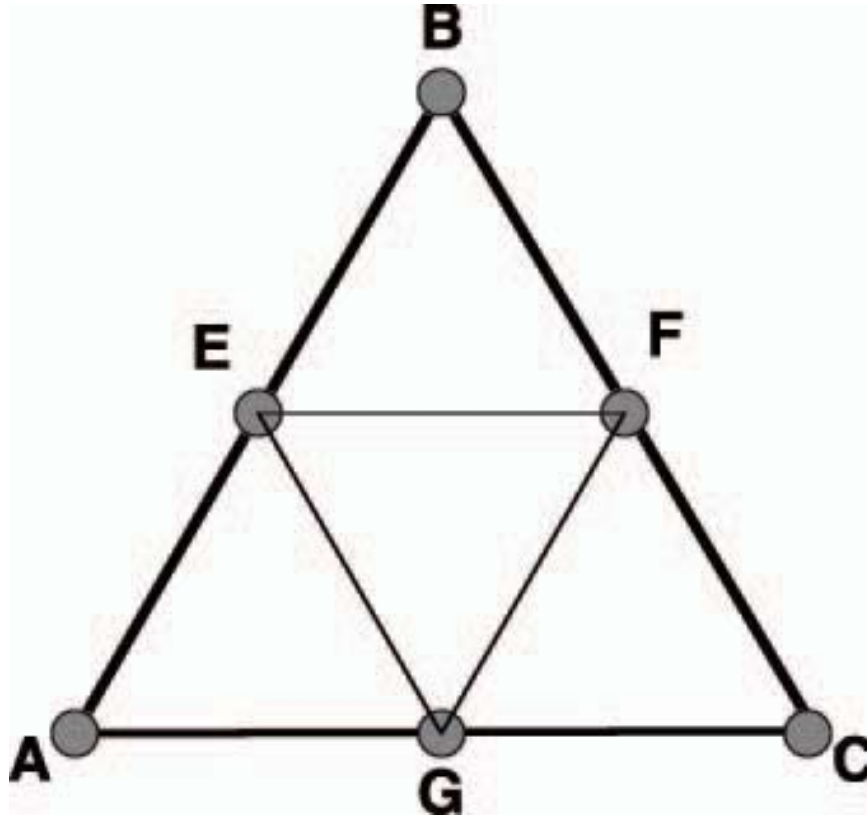


FIGURE 3. An example of the geodesic split. The midpoints of geodesics  $AB$ ,  $BC$ , and  $CA$  are added as the points  $E$ ,  $F$ , and  $G$  respectively, and then the edges  $EF$ ,  $FG$ , and  $GE$  are added.

**4.3. Geodesic Words.** By applying the centroid and geodesic splittings repeatedly from an original shape a family of related polyhedrons may be constructed. Letting  $C$  stand for a centroid split and  $G$  stand for a geodesic split one can construct a geodesic word from a basic polyhedron to much moer complex shapes.

**Definition 4.** *A Geodesic Word is a string of  $C$  and  $G$  operations representing the repeated splitting of faces of a basic polyhedron.*

As example the word  $CCCG$  represents three centroid splits and then a geodesic split from one of the original polyhedrons.

**4.4. Vertex Degrees by Voronoi Methods.** A well-known result in the study of polyhedrons [14] composed primarily of triangle and square faces relates the number of vertices and their degrees together, and holds

$$2v_4 + v_5 - v_7 - 2Q = 12 \quad (7)$$

where  $v_4$  is the number of vertices of degree four,  $v_5$  the number of vertices of degree five,  $v_7$  the number of vertices of degree seven, and  $Q$  the number of square faces.

In applying the geodesic splitting of a face vortices of only degree six are created, and so the new polyhedron satisfies without effort into the above relationship. In

the centroid split, however, the degrees of all existing vertices are doubled, and a number (equal to the number of faces in the polyhedron being split) of new vertices of degree three are created, resulting in a shape which does not immediately fit this relationship at all.

Therefore if the count of vertex degrees is of interest – though for mechanical properties such as the system’s potential energy it is not, since the edges however drawn do not change the locations of vertices and therefore do not affect the mechanics at all – either the relationship of equation 7 must be abandoned or one must redraw vertex edges after each centroid split. If the edge lines are redrawn, and new triangular faces created, a regular algorithm for such redrawing is necessary. One satisfactory algorithm is to use a method based on Voronoi diagrams.

**Definition 5.** *A vertex degree, after redrawing, is equal to the degree of the polygon which surrounds that vertex once the Voronoi diagram based on the set of all the polyhedron’s vertices has been drawn.*

A Voronoi diagram takes a base set of  $N$  points and divides the domain into  $N$  regions, each of which consists of the points closest to exactly one point of the original base set. The boundaries of these regions will be polygons, in this case on the surface of the sphere.

Draw an edge from point  $\vec{x}_i$  to  $\vec{x}_j$  if and only if the region surrounding  $\vec{x}_i$  is adjacent to that surrounding  $\vec{x}_j$ . This new set of edges based on the centroid algorithm restores the vertices which had originally been degree five to that degree again, restores those which had been degree six to that again, and sets the new vertices to degree six. As a result the relationship 7 again.

This method breaks down, by creating nontriangular faces, if two or more adjacent faces of the split polyhedron are coplanar. Effectively if the figure has a nontriangular face the Voronoi-based redrawing of edges will propagate that non-triangular face.

**4.5. Noncommutivity of C and G operations.** A cursory examination of the the result of words  $CG$  and of  $GC$  on any triangle face suggests the operations may commute. In either order the original face is split into ten points, and drawing the effects of these operations on a planar triangle reinforces this suggestion.

**Theorem 1.** *For a triangle resting in the plane, the centroid split and the geodesic split of that triangle are commutative operations.*

*Proof.* Let triangle  $ABC$  rest in the plane. A centroid split creates the point  $D$  and the edges  $AD$ ,  $BD$ , and  $CD$ . The geodesic split of this creates point  $E$  bisecting  $AB$ , point  $F$  bisecting  $BC$ , point  $G$  bisecting  $CA$ , point  $H$  bisecting  $AD$ , point  $I$  bisecting  $BD$ , and point  $J$  bisecting  $CD$ .

Now consider the geodesic split followed by the centroid split. Again on triangle  $ABC$ , let point  $E'$  bisect  $AB$ ,  $F'$  bisect  $BC$

$D' \sim D$  as the triangle  $E'F'G'$  is similar to  $ABC$ , with edge  $E'F'$  parallel to  $AB$ ,  $F'G'$  parallel to  $BC$ , and  $G'E'$  parallel  $CA$ .  $H' \sim H$  because  $AE'G'$  is similar to  $ABC$ , with the length  $AE'$  half that of  $AB$  (and so on), therefore the distance from  $A$  to the centroid  $H'$  is half the distance from  $A$  to the centroid  $D'$ . By similar arguments  $I' \sim I$  and  $J' \sim J$ .

Thus on the plane the centroid and geodesic splittings of a triangle commute in their placement of points. ■

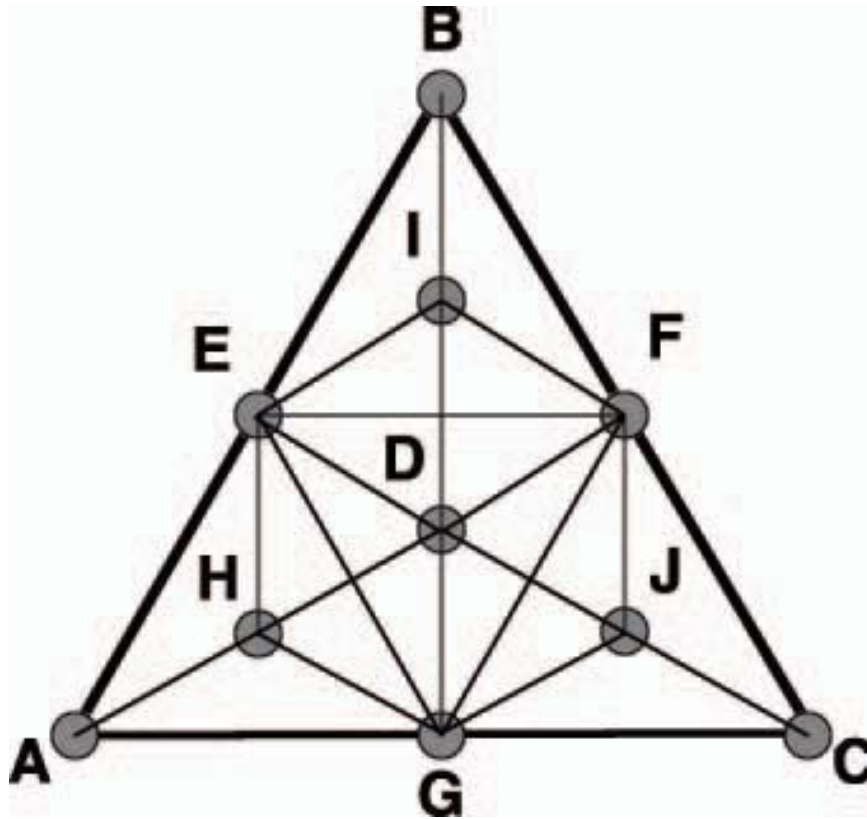


FIGURE 4. An illustration of how the centroid and geodesic splits may be expected to commute. As constructed on the plane the triangle  $AEG$  must be similar to  $ABC$  (and similarly  $EBF$  and  $GFC$  are also similar to  $ABC$ ), making it possible to show the centroid and geodesic operations may be performed in either order. However, similar triangles do not exist on the surface of the sphere and so the proof breaks down. Figure 5 provides an example of the  $CG$  word resulting in different points than the  $GC$  word does.

**Corollary 2.** *For a spherical triangle the centroid and geodesic splittings do not commute.*

*Proof.* Commutativity hold for triangles on the surface of the sphere, which form the geometry used in these polyhedron splittings. Critical to the proof of the commutivity in the plane is the use of similar triangles to show the equal positioning of points  $H$  and  $H'$ , of  $I$  and  $I'$ , and of  $J$  and  $J'$ . Similar triangles do not exist on the surface of the sphere and as a result the proof does not hold – and in practice an examination of the difference between  $CG$  and  $GC$  starting from a simple polyhedron shows this. Figure 5 shows an example of these noncommuting operations. While the graphs of vertex positions may not be obvious, the differences between their radial distribution functions demonstrate they can not be equivalent configurations: one is not a rotation or reflection of the other. ■

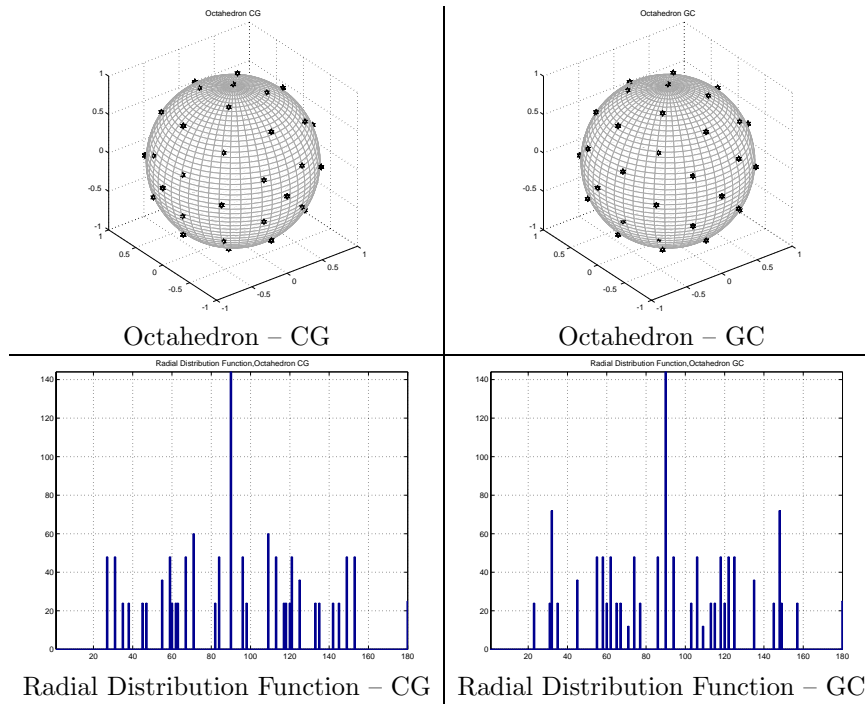


FIGURE 5. The octahedron split first by the geodesic word  $GC$  and then by the word  $CG$ , showing the final polyhedrons to not be identical.

It is worth noting that as the area of a spherical triangle decreases – as the triangle gets closer to being planer – the centroid and geodesic splits come closer to commuting, in that the results of a  $CG$  and of a  $GC$  operation result in sets of points which are closer to one another. This is ultimately reflected numerically in the energies of polyhedrons split by long geodesic words begin to vary only slightly when they differ only in the last two letters – and this does not necessarily take many splits. Words as short as three letters can see their last two letters come near commuting.

**4.6. Polyhedron Trees.** From any reference base polyhedron which has only triangular faces one can perform geodesic word splittings on each of the faces. If they are on the surface of the sphere then every geodesic word represents a new polyhedron. As each split may be either a centroid or a geodesic split, the structure of a binary tree is suggested, each geodesic word corresponding to one branch.

**Definition 6.** A *Polyhedron Tree* is the binary tree constructed by taking a polyhedron base and applying to it all geodesic words.

One may build a tree of polyhedrons belonging to one of several families and so covering a great number of possible numbers of vertices. Although the number of geodesic and centroid splits in a word defines the number of vertices which will arise from that splitting being performed on a basic shape, the noncommutivity of those operations on the surface of the sphere results in distinct polyhedrons for each case.

Word	Tetrahedron	Octahedron	Icosahedron
Base Shape	4	6	12
C	8	14	32
G	10	18	42
CC	20	38	92
CG	26	50	122
GC	26	50	122
GG	34	66	162
CCC	56	110	272
CCG	74	146	362
CGC	74	146	362
CGG	98	194	482
GCC	74	146	362
GCG	98	194	482
GGC	98	194	482
GGG	130	258	642
CCCC	164	326	812
CCCG	218	434	1082
CCGC	218	434	1082
CCGG	290	578	1442
CGCC	218	434	1082
CGCG	290	578	1442
CGGC	290	578	1442
CGGG	386	770	1922
GCCC	218	434	1082
GCCG	290	578	1442
GCGC	290	578	1442
GCGG	386	770	1922
GGCC	290	578	1442
GGCG	386	770	1922
GGGC	386	770	1922
GGGG	514	1026	2562

FIGURE 6. Vertex counts for geodesic word splittings from several polyhedron bases. The number of vertices, as well as the numbers of faces and edges, may be derived from formulas 5 and 6.

For the first generations of polyhedrons split off the base polyhedra of the tetrahedron, octahedron, and icosahedron one has this table of vertex counts for the words of length up to four:

The table can clearly be extended indefinitely, with the words of length  $n$  generating  $2^n$  unique vertex configurations, but only  $n + 1$  distinct numbers of vertices. Although in the first few branches of this tree it is not observed that any number  $N$  may be generated by two geodesic words which have different numbers of centroid and geodesic splits (whether working from the same or different base polyhedra), it is not asserted that any given number may be generated from at most one base polyhedron and number of centroid and geodesic splits.

Several polyhedra of interest are generated by these branches: the tetrahedron split by  $C$ , for example, is the cube, and the icosahedron split by  $C$  is the truncated icosahedron (and its own dual). Extremely few of these polyhedra are known “interesting” configurations such as Platonic or Archimedean solids.

Symmetry considerations lead one to expect the basic shapes of the tetrahedron, octahedron, and icosahedron will represent equilibrium configurations for the vortex problem – vortices placed at the vertices of these polyhedra on the unit sphere will remain in place. Similarly one expects any number of purely geodesic splits, or a chain of geodesic splits followed by one centroid split, to produce another equilibrium.

**5. Numerical Results.** Examined in this section is the agreement between the results of the Monte Carlo algorithm and the configuration of several known polyhedron vertices. Initial successes in matching the configurations of points for shapes such as the tetrahedron and the octahedron suggest regular polyhedrons may represent extremal states for the problem of vortices on the surface of the sphere. This is however not the case, as examination of the problem with 8 vortices demonstrates – the rectangular antiprism is a shape with a lower energy than the cube has.

The numerical results derived here were run for 40,000 sweeps of the particles, with an inverse temperature  $\beta$  of 100,000,000. The maximum angle by which any vortex was allowed to move was 0.05 radians. The random number seed used was the time of day, and the calculations performed by computers running Matlab (and reliant upon its built-in random number sequence generator). The source codes are available upon request.

The first subsections of each of these configurations is the result not of a Monte Carlo simulation, but rather the result of using the precise coordinates of the vertices of a polyhedron as derived by performing the specified splits on the faces of the tetrahedron, octahedron, or icosahedron. The use of these shapes for reference validates the routines which calculate system energy, radial distribution function, and which plot the positions of these points. The maps of the plots are an unprojected latitude-longitude system, unfortunately distorting to an extent the angles between vortex pairs and occasionally making a configuration difficult to identify, as in sections 6.1.1 and 6.1.2 in which both graphs displaying the same state is not immediately obvious.

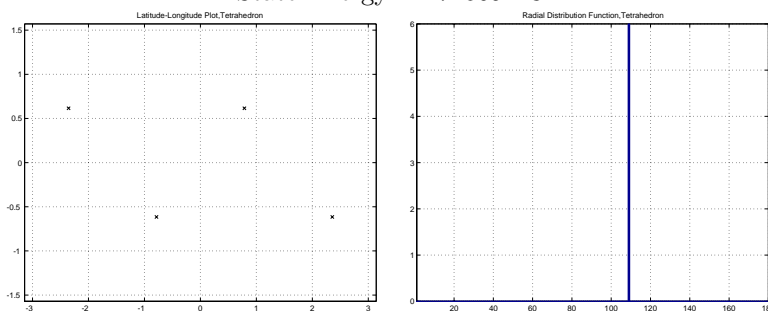
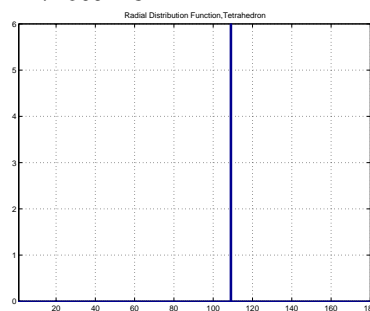
Each final subsection is the result of a Monte Carlo simulation on the corresponding number of vortices along with the energy of that state. This is expected to be at or near the extremal state energy for the corresponding number of vortices due to the ability of the Monte Carlo algorithm to escape local energy minimums and find eventually the global minimum.

## 6. The Tetrahedron Tree.

### 6.1. Four Points.

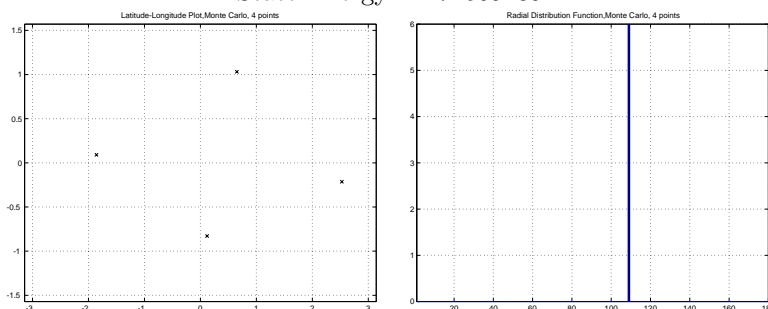
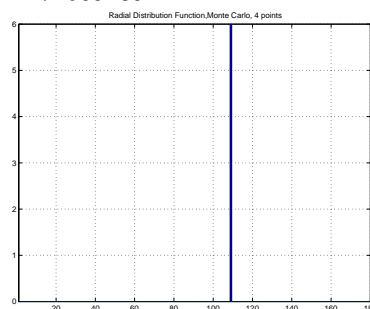
6.1.1. *Tetrahedron.* The tetrahedron is one of the Platonic solids [5] and is a commonly recognized shape. In the vortex problem it is a dynamic equilibrium.

State Energy: -1.72609243

Latitude-Longitude Map  
Figure 6.1.1aRadial Distribution Function  
Figure 6.1.1b

6.1.2. *Free Particles.* Four particles find the tetrahedron. As the Monte Carlo algorithm has no means of detecting latitude the configuration is 'pointed' in a randomly chosen direction. Because of this, and the distortion of angles and areas forced by projecting the surface of the sphere onto the latitude-longitude rectangle plotted, the tetrahedron is not obvious as plotted (as several other shapes will not be obvious from their plots, as in sections 7.1.2 and 6.2.2). The energy and radial distribution function indicate the tetrahedron has been found.

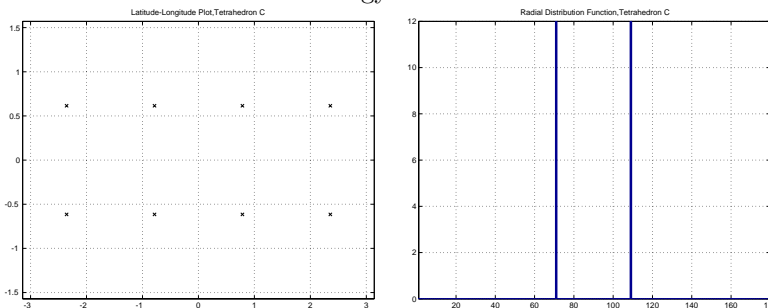
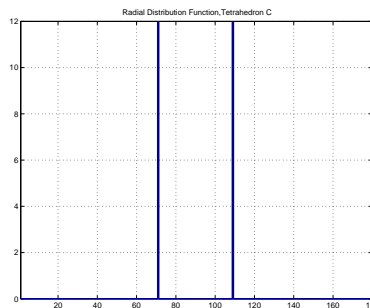
State Energy: -1.72609239

Latitude-Longitude Map  
Figure 6.1.2aRadial Distribution Function  
Figure 6.1.2b

## 6.2. Eight Points: Single-Letter Words.

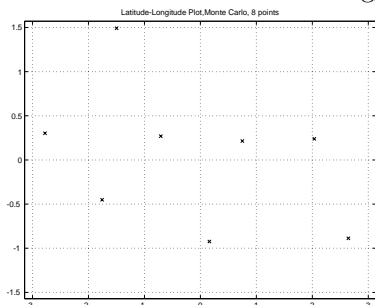
### 6.2.1. *C Split.*

State Energy: -1.35919229

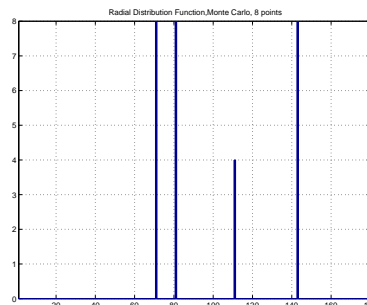
Latitude-Longitude Map  
Figure 6.2.1aRadial Distribution Function  
Figure 6.2.1b

6.2.2. *Free Particles.*

State Energy: -1.44791144



Latitude-Longitude Map  
Figure 6.2.2a

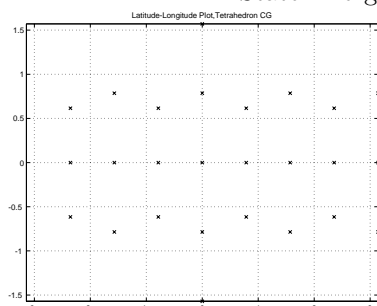


Radial Distribution Function  
Figure 6.2.2b

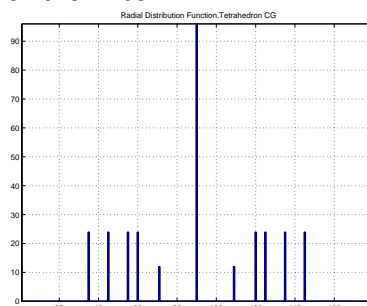
6.3. 26 Points: Two-Letter Words.

6.3.1. *CG Split.*

State Energy: 52.04024268



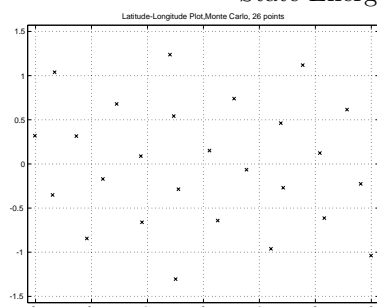
Latitude-Longitude Map  
Figure 6.3.1a



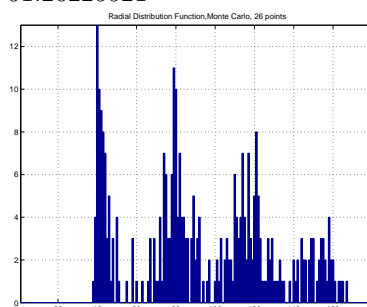
Radial Distribution Function  
Figure 6.3.1b

6.3.2. *Free Particles.*

State Energy: 51.26225521



Latitude-Longitude Map  
Figure 6.3.2a

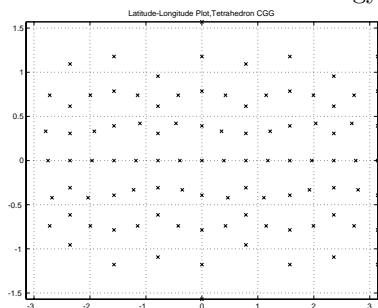
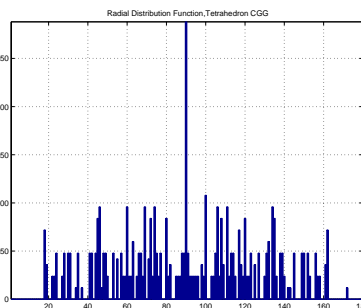


Radial Distribution Function  
Figure 6.3.2b

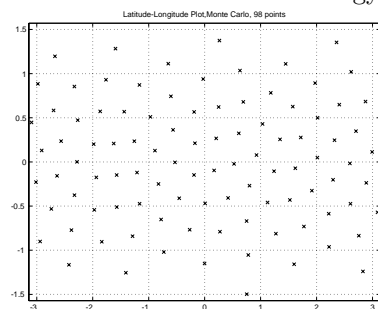
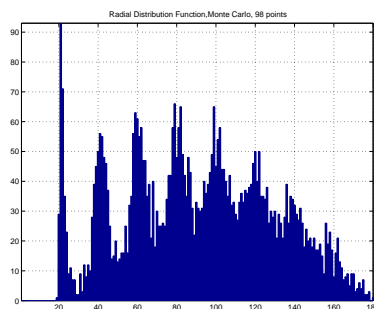
6.4. 98 Points: Three-Letter Words.

6.4.1. *CGG Split.*

State Energy: 1218.58714521

Latitude-Longitude Map  
Figure 6.4.1aRadial Distribution Function  
Figure 6.4.1b6.4.2. *Free Particles.*

State Energy: 1210.13160347

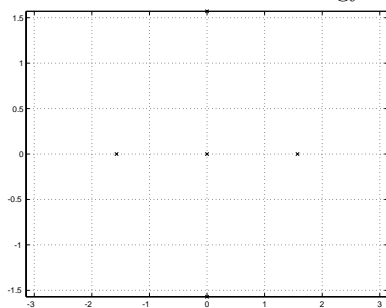
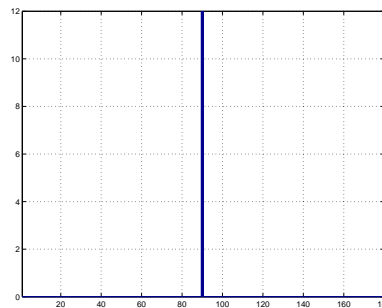
Latitude-Longitude Map  
Figure 6.4.2aRadial Distribution Function  
Figure 6.4.2b

## 7. The Octahedron Tree.

## 7.1. Six Points.

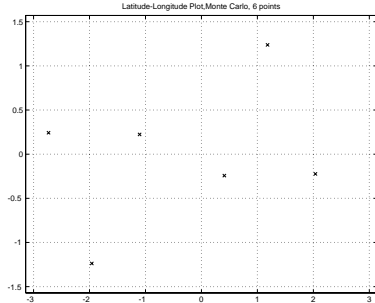
7.1.1. *Octahedron.* The octahedron is another Platonic solid. It is clearly an equilibrium and the evidence of Monte Carlo experiments (section 7.1.2) indicates it is also an energy minimum.

State Energy: -2.07944154167984

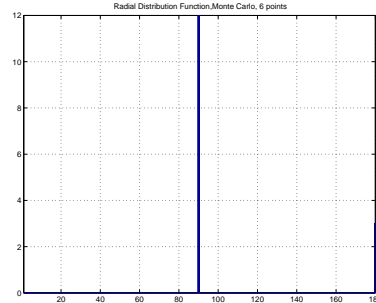
Latitude-Longitude Map  
Figure 7.1.2aRadial Distribution Function  
Figure 7.1.2b

7.1.2. *Free Particles.* Six free particles move towards the extremal state, which is the octahedron configuration seen in section 7.1.2.

State Energy: -2.07944143162953



Latitude-Longitude Map  
Figure 7.1.2a

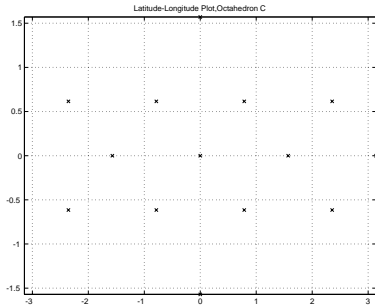


Radial Distribution Function  
Figure 7.1.2b

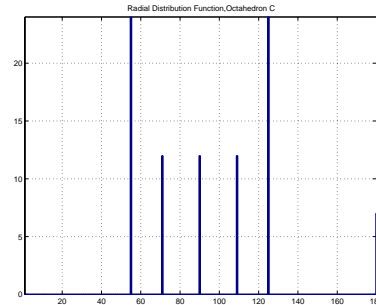
7.2. 14 Points: Single-Letter Words.

7.2.1. *C Split.*

State Energy: 6.29252876



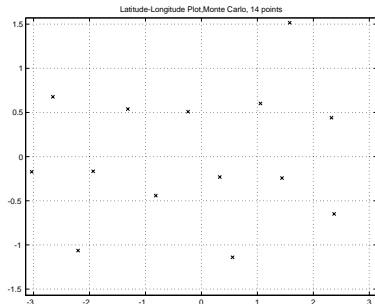
Latitude-Longitude Map  
Figure 7.2.1a



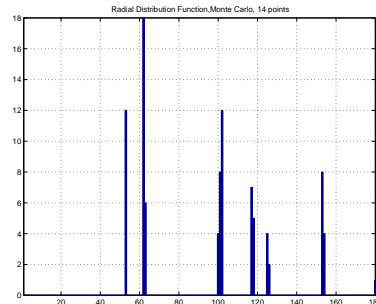
Radial Distribution Function  
Figure 7.2.1b

7.2.2. *Free Particles.*

State Energy: 6.26082162



Latitude-Longitude Map  
Figure 7.2.2a

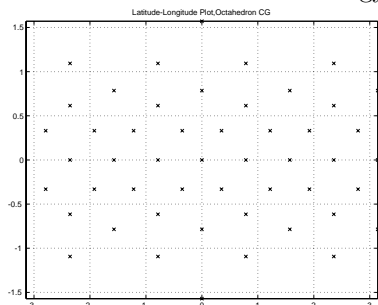
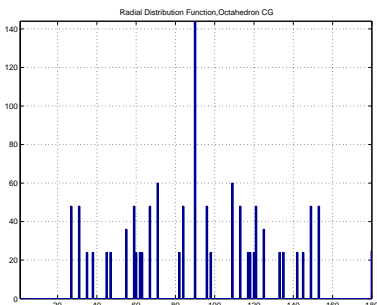


Radial Distribution Function  
Figure 7.2.2b

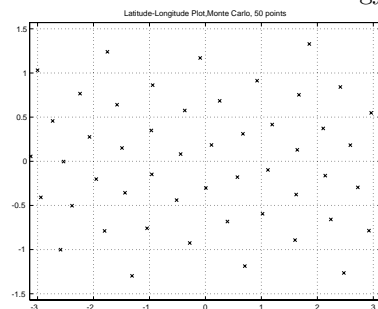
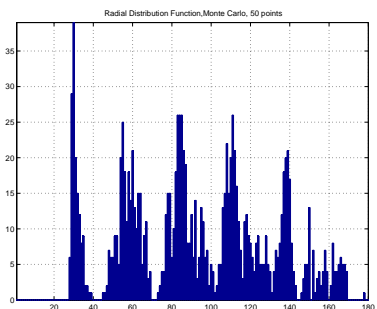
7.3. 50 Points: Two-Letter Words.

7.3.1. *CG Split.*

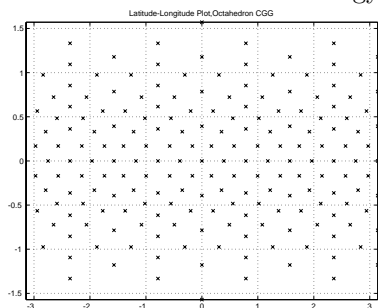
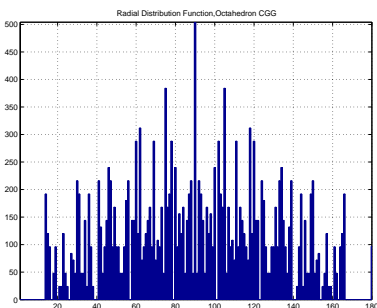
State Energy: 266.54209732

Latitude-Longitude Map  
Figure 7.3.1aRadial Distribution Function  
Figure 7.3.1b7.3.2. *Free Particles.*

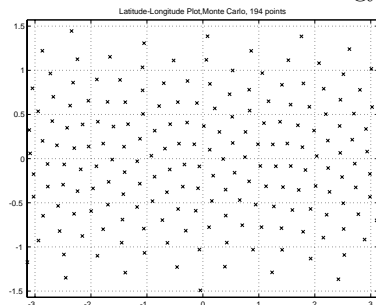
State Energy: 266.05829961

Latitude-Longitude Map  
Figure 7.3.2aRadial Distribution Function  
Figure 7.3.2b7.4. **194 Points: Three-Letter Words.**7.4.1. *CGG Split.*

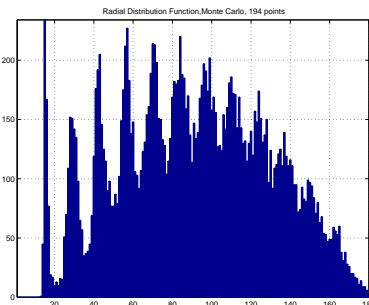
State Energy: 5192.17477404

Latitude-Longitude Map  
Figure 7.4.1aRadial Distribution Function  
Figure 7.4.1b7.4.2. *Free Particles.*

State Energy: 5186.55694273



Latitude-Longitude Map  
Figure 7.4.2a



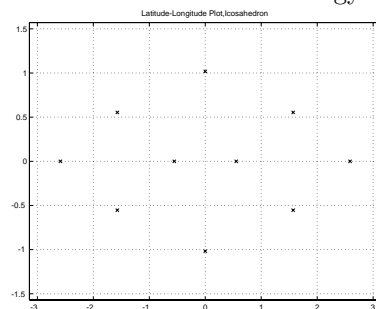
Radial Distribution Function  
Figure 7.4.2b

## 8. The Icosahedron Tree.

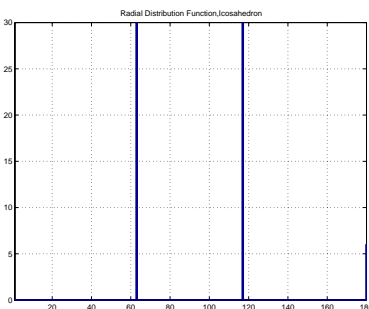
### 8.1. 12 Points.

8.1.1. *Icosahedron.* With twelve vortices one has two polyhedron configurations as provided by Coxeter's array of Platonic solids and their duals [5]. The first of these is the icosahedron. The icosahedron is not the only configuration of twelve vortices with analytically known points; another configuration is the cuboctahedron. The cuboctahedron is not found by a Monte Carlo experiment with free particles.

State Energy: 2.53542345606662



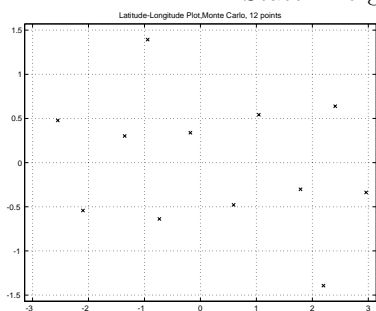
Latitude-Longitude Map  
Figure 8.1.1a



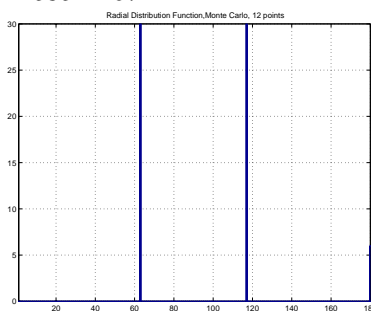
Radial Distribution Function  
Figure 8.1.1b

8.1.2. *Free Particles.* Twelve free particles move towards the icosahedron shape. Though the latitude-longitude plots are not obviously identical, their radial distribution functions match precisely and their energies are very nearly equal.

State Energy: 2.53542467



Latitude-Longitude Map  
Figure 8.1.2a

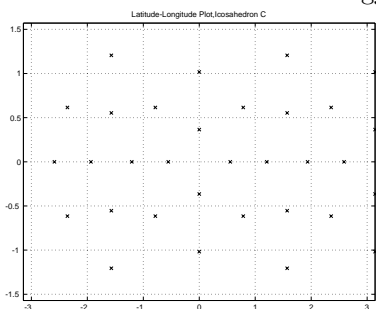


Radial Distribution Function  
Figure 8.1.2b

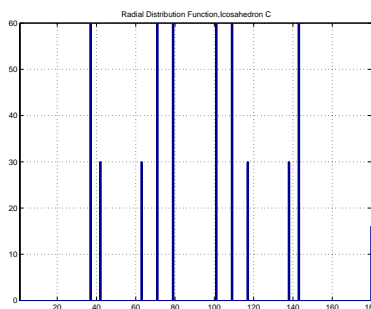
8.2. 32 Points: Single-Letter Words.

8.2.1. *C Split.*

State Energy: 89.04326633



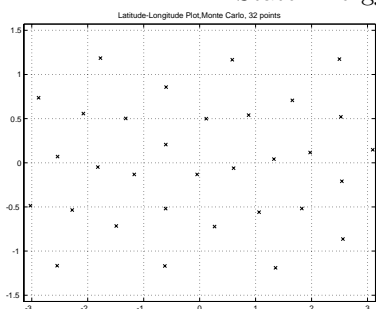
Latitude-Longitude Map  
Figure 8.2.1a



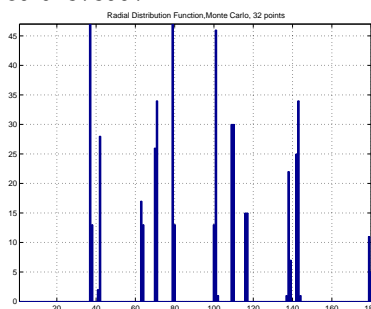
Radial Distribution Function  
Figure 8.2.1b

8.2.2. *Free Particles.*

State Energy: 89.04373997



Latitude-Longitude Map  
Figure 8.2.2a

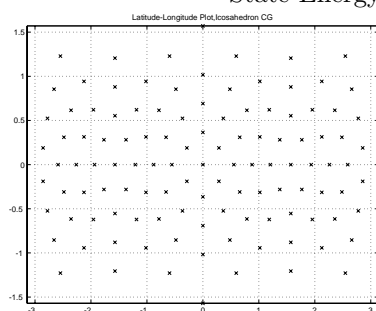


Radial Distribution Function  
Figure 8.2.2b

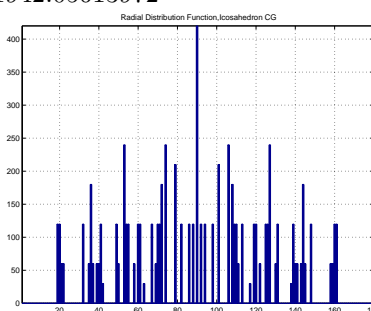
8.3. 122 Points: Two-Letter Words.

8.3.1. *CG Split.*

State Energy: 1942.05613972



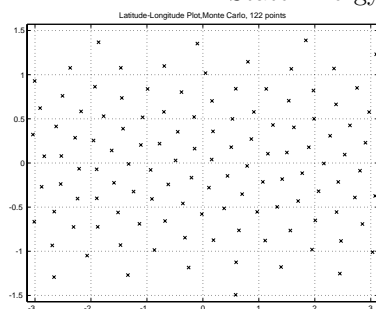
Latitude-Longitude Map  
Figure 8.3.1a



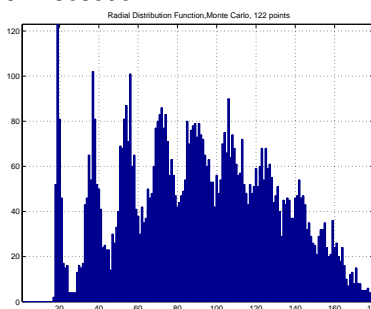
Radial Distribution Function  
Figure 8.3.1b

8.3.2. *Free Particles.*

State Energy: 1942.36355642



Latitude-Longitude Map  
Figure 8.3.2a

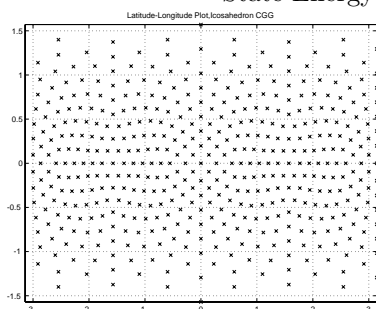


Radial Distribution Function  
Figure 8.3.2b

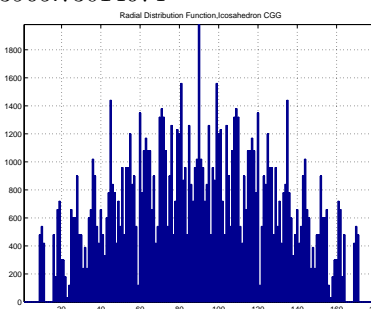
8.4. **482 Points: Three-Letter Words.**

8.4.1. *CGG Split.*

State Energy: 33965.73014674

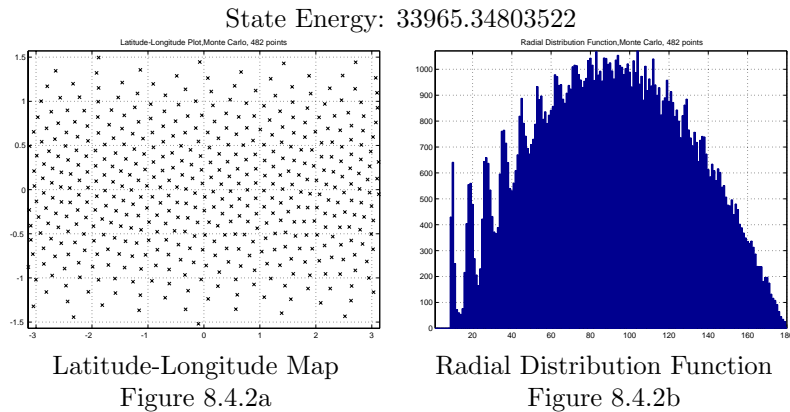


Latitude-Longitude Map  
Figure 8.4.1a



Radial Distribution Function  
Figure 8.4.1b

8.4.2. *Free Particles.*



## 9. Polyhedron Results.

**9.1. Split Polyhedrons and Extremal States.** The vortex interaction energy, as one expects from considerations of the mean field theory – or simply from observing that the number of particles is increasing and therefore the number of pairs increasing as the square of the number of points [2] – grows quadratically in terms of the number of vortices. This growth is independent of whether the vortices are arranged at the vertices of a polyhedron or whether they are allowed to find an extremal state by the Monte Carlo algorithm, as indicated by figures 7 and 8.

The tables in this section present the minimum states for the first few lengths of geodesic words based on the polyhedrons of the tetrahedron, the octahedron, and the icosahedron. These figures, each Platonic solids with faces composed of triangles (with vertices uniformly of degree three, four, and five, respectively) and so enjoy considerable rotational symmetry. They are also known to be extremal states for their corresponding vortex problem and are dynamic equilibriums. In each table the starting polyhedron and the geodesic word used to generate a configuration of  $N$  points is given, and the energy of the polyhedron as generated by that geodesic word is provided and compared to the energy of the extremal state as found by the Monte Carlo method (section 2.1).

The polyhedron-based energies and the Monte Carlo extremal state energies disagree in almost every case besides the basic polyhedrons. Several polyhedron configurations approach the Monte Carlo energy closely, and in one case – the Icosahedron split by  $CG$  – the polyhedron energy is below that of the Monte Carlo energy. This reflects that the Monte Carlo algorithm does quickly reach a point near the energy minimum, but is slow to then reach exactly the energy minimum. There is a relatively small region of phase space which needs to be reached, and a finite run may nevertheless not be long enough to reach it. In support of that argument one notes the Monte Carlo extremal state energy for the tetrahedron, octahedron, and icosahedron are very slightly higher than the polyhedron ideals, though the Monte Carlo extremal states are extremely near the geodesic word-generated positions.

In the polyhedrons grown from the octahedron the agreement between polyhedron energies of longer words as the final geodesic letters are reversed grows slightly better. In the shapes grown from the icosahedron even the  $CG$  word has an agreement in energies about a tenth of a percent to the Monte Carlo-generated extremal state energy. The  $CGG$  state does not agree as tightly with the extremal state energy, but it is still in excellent agreement.

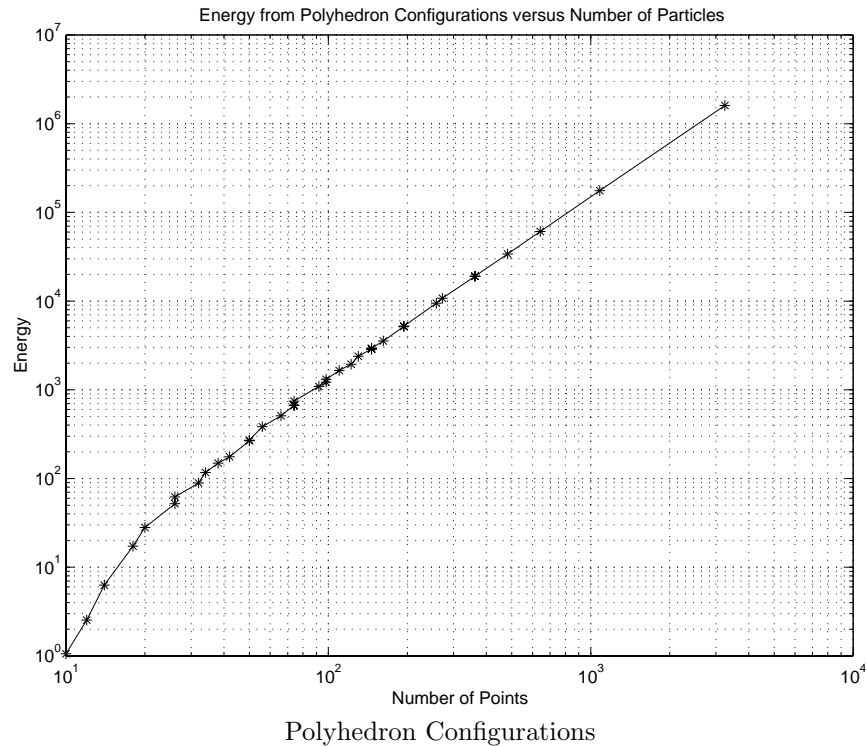


FIGURE 7. The system energy as a function of the number of particles for the examined polyhedrons.

The radial distribution function as generated by the Monte Carlo routine is closer to a uniform distribution – note that the distribution is close to a sinusoidal curve – whereas the radial distribution functions for polyhedrons generated by geodesic words have fewer and rarer peaks, a much more crystalline configuration.

**9.2. Pairwise Interaction Energies.** From observing that the energy of the system grows as the square of the number of particles (as derived by Bergersen et al [2]) – that is, the number of pairs of particles in the system – the question of what the average energy of interaction of a pair might be is raised. Figures 9 and 10 and the tables in this subsection represent the energies of the system divided by  $N(N - 1)$ , both for the polyhedrons as generated by the geodesic trees grown from the tetrahedron, octahedron, and icosahedron, and for the Monte Carlo extremal state energy found for the corresponding number of points.

As may be expected from the quadratic growth of energy terms, once the number of points grows moderately large, the pairwise energy appears to approach a constant approximately 0.15. As may be expected from the relatively low variation in system energies despite the noncommutivity of centroid and geodesic splits the pairwise energy depends only slightly on the geodesic word.

The pairwise Monte Carlo energy tends to have a slightly lower value than that of the polyhedron-based configuration.

It is clear that for any finite number of vortices the system energy – and thus the pairwise energy – may be made arbitrarily large, by the expedient of moving at

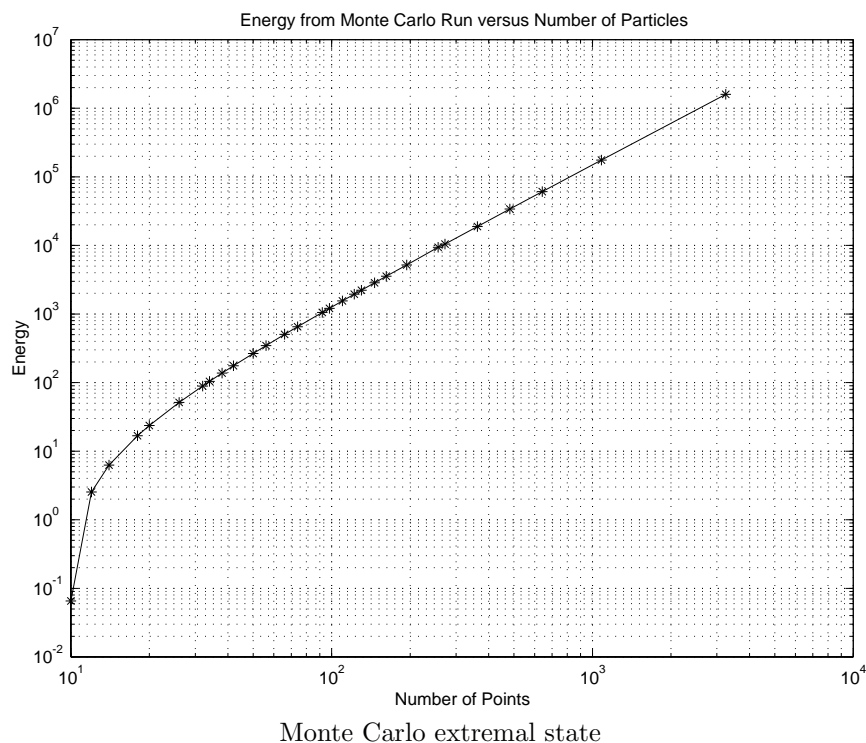


FIGURE 8. The system energy as a function of the number of particles for the extremal state as found by a Monte Carlo algorithm.

	N	Polyhedron Energy	Monte Carlo Energy
Tetrahedron	4	-1.72609243	-1.72609239
C	8	-1.35919229	-1.44791144
CG	26	52.04024268	51.26225521
CGG	98	1218.58714521	1210.13160347

	N	Polyhedron Energy	Monte Carlo Energy
Octahedron	8	-2.07944154	-2.07944143
C	14	6.29252876	6.26082162
CG	50	266.54209732	266.05829961
CGG	194	5192.17477404	5186.55694273

	N	Polyhedron Energy	Monte Carlo Energy
Icosahedron	12	2.53542346	2.53542467
C	32	89.04326633	89.04373997
CG	122	1942.05613972	1942.36355642
CGG	482	33965.73014674	33965.34803522
CCGC	1082	176215.65351546	175409.18318903
CCCCG	3242	1602250.21172894	1598209.70411300

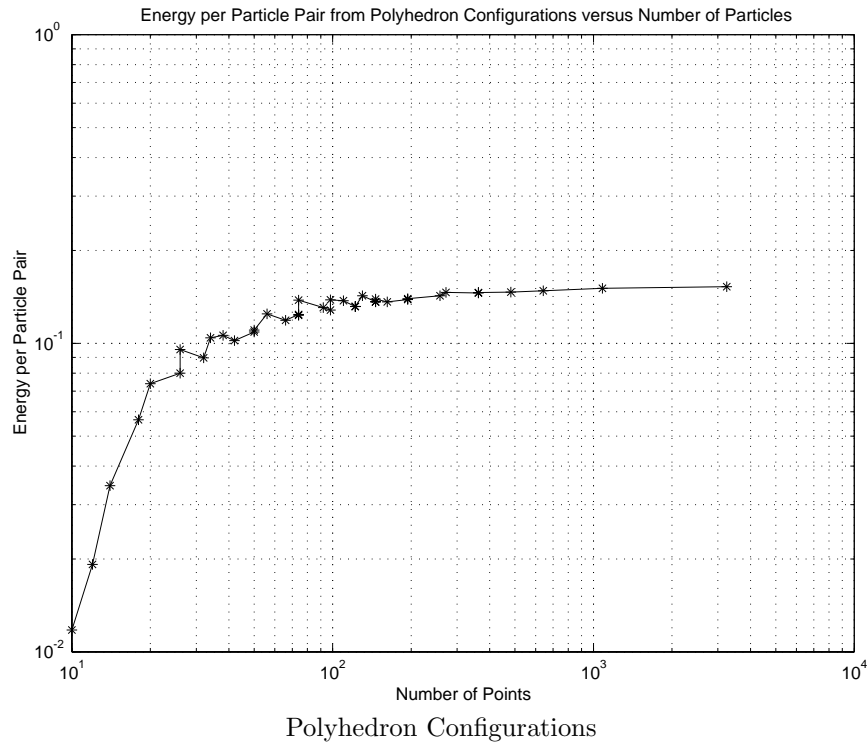


FIGURE 9. The system energy per number of pairs as a function of the number of particles for the examined polyhedrons.

least one pair of vortices sufficiently close together. This indicates that though both polyhedrons (of many different shapes) and Monte Carlo based extremal states tend towards a very uniform finite pairwise energy, this pairwise energy does nevertheless depend in some way on the distribution of points. It is not simply the case that as the number of points grows arbitrarily large the pairwise energy will approach approximately 0.15.

As shown in section 3, the energy per pair of particles approaches a mean field value of  $-\frac{1}{2}(\log(2) - 1)$  as the number of particles grows without bound, and this appears to be the limit reached by both the Monte Carlo-derived extremal state and by the polyhedron configurations developed by the geodesic words from the basic shapes.

**9.3. Energy Overage.** In this subsection, figure 11, and the corresponding tables represent the energy ‘overage,’ the amount by which the energy of the polyhedron configuration exceeds the Monte Carlo extremal state energy. With the exceptions of the base states of the tetrahedron, octahedron, and icosahedron – and the exceptional case mentioned in section 9.1 of the icosahedron split by the geodesic word *CG* – these overages are all positive. The polyhedron energies are greater than the Monte Carlo extremal state energies.

Several of the values for low numbers of vortices return negative numbers, reflecting only that the Monte Carlo extremal state energies were negative, and so the fraction of the polyhedron energy minus Monte Carlo energy over the Monte

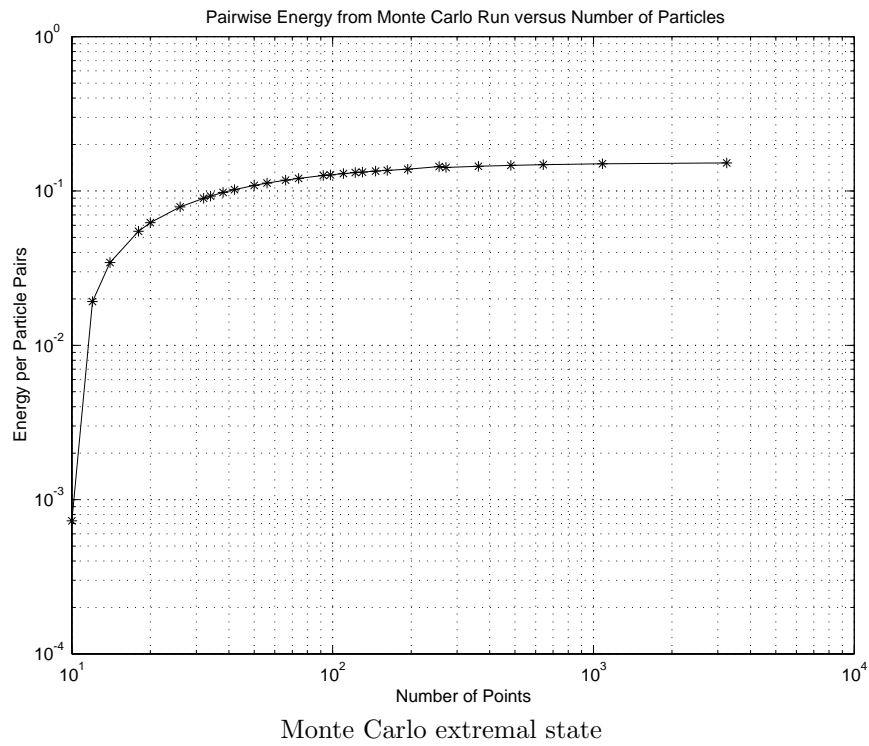


FIGURE 10. The system energy per number of pairs as a function of the number of particles for the extremal state as found by a Monte Carlo algorithm.

	N	Pairwise Polyhedron	Pairwise Monte Carlo
Tetrahedron	4	-0.14384103583	-0.1438410325
C	8	-0.02427129089	-0.02585556143
CG	26	0.08006191182	0.07886500802
CGG	98	0.12819136811	0.12730187287

	N	Pairwise Polyhedron	Pairwise Monte Carlo
Octahedron	6	-0.06931471133	-0.06931471433
C	14	0.03457433385	0.03440011879
CG	50	0.10879267238	0.10859522433
CGG	194	0.13867247407	0.13852243317

	N	Pairwise Polyhedron	Pairwise Monte Carlo
Icosahedron	12	0.01920775348	0.01920776265
C	32	0.08976135719	0.08976183465
CG	122	0.13155779296	0.13157861783
CGG	482	0.14650378338	0.14650213523
CCGC	1082	0.15065776837	0.14996826652
CCCGC	3242	0.15248892265	0.15210438056

	N	Energy Overage		N	Energy Overage
Tetrahedron	4	0.00000002317	Octahedron	6	-0.00000004328
C	8	-0.06127387874	C	14	0.00506437364
CG	26	0.01517661419	CG	50	0.00181820192
CGG	98	0.00698729106	CGG	194	0.00108315234

	N	Energy Overage
Icosahedron	12	-0.00000047724
C	32	-0.00000531918
CG	122	-0.00015826939
CGG	482	0.00001125004
CCGC	1082	0.00459765168
CCCGC	3242	0.00252814609

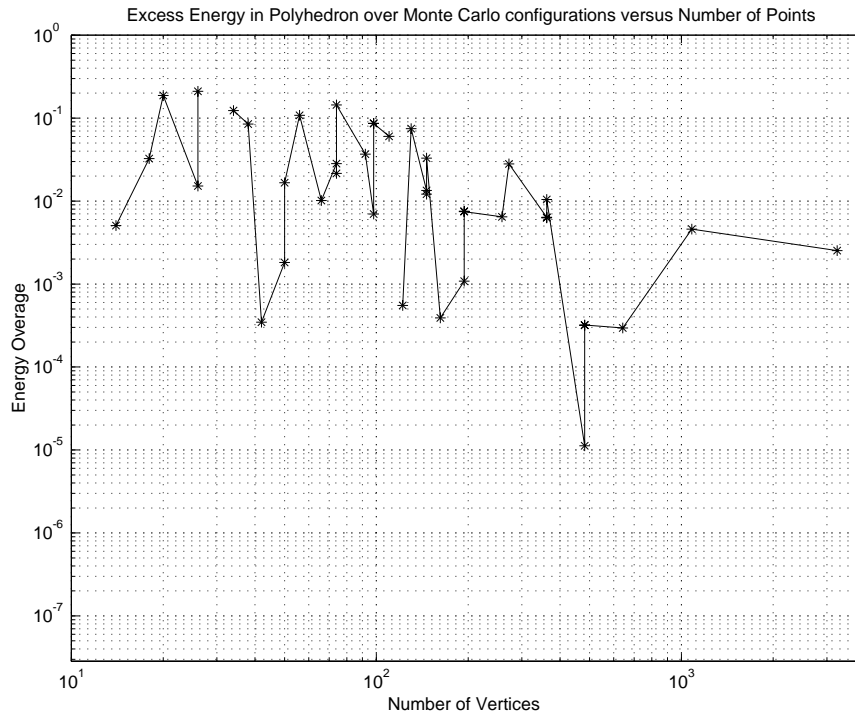


FIGURE 11. The percentage by which polyhedron energies exceed the Monte Carlo-generated extremal state energies as a function of the number of particles.

Carlo energy is negative. Similarly – as the Monte Carlo extremal state energy is negative for the tetrahedron extremal state – the ‘overage’ is recorded as positive even though the Monte Carlo extremal state is marginally higher than the analytically determined tetrahedron coordinates. The exceptionally high overage from the tetrahedron split by  $G$  is reflective of the Monte Carlo energy being a small number, magnifying the size of a difference which is not much greater than that of the tetrahedron split by  $C$ .

As a function of word length the energy overage appears to decline as either the number of points grows greater or the word length increases – since the traits are correlated the available data does not distinguish between the two. The available numerical experiments do not form a clear body of evidence indicating the difference between polyhedron energies and Monte Carlo extremal state energies will become arbitrarily small as the number of points increases. The observations of sections 9.1 and 9.2 indicating the steady growth of energy with the number of points suggests only that the energies of polyhedrons and of the extremal states should grow at the same rates with the number of points.

**10. Conclusions.** The traditional use of a Monte Carlo algorithm to find statistical equilibriums extends easily to finding the energy minimum for an  $N$ -body problem. Such Monte Carlo approaches provide a computationally rapid method of reaching a configuration of points which is close to the extremal state for, in this case, the logarithmic potential. It has weaknesses in locating the precise coordinates of a extremal state, but the ease of implementation and speed of producing approximate results leaves it still a potent tool.

The radial distribution function is a convenient tool to determine quickly that two configurations of points on the sphere are not equivalent, as was done in showing that the centroid and geodesic splits on the sphere do not commute. It is not asserted that the radial distribution function can be used to prove two configurations are equivalent, but the ability to rule out apparent equivalences is itself of interest, and the extension of the radial distribution function to determining any pairwise-defined function, such as potential energy, suggests the function may have considerable utility.

Polyhedrons may be constructed as the ‘splittings’ of simpler polyhedrons, and the construction of complex shapes from simple polyhedrons known to be of interest results in shapes which may have considerable structure – with many points near one another or confined to a relatively small portion of the sphere, configurations far from homogenous – yet without the energy growing more than marginally greater than what the Monte Carlo algorithm suggests is the global energy minimum. How other splitting operations may fit into this sort of algorithm, both to generate polyhedrons and how well their energies fit those of the Monte Carlo and the centroid and geodesic splits, is an interesting question deserving of exploration.

The plots of energy per particle pair in figures 9 and 10 agree with the calculation of Bergersen et al [2] that a mean field limit for the energy of this logarithmic interaction can be expected to hold, even though as Bergersen et al calculate the standard thermodynamic limit is found not to be valid.

The ability of Monte Carlo algorithms to generate states near an equilibrium, either for the case of free particles or for constrained particles, offers avenues for further research in pairwise interactions and will be examined in a coming paper [11]. Similarly the use of geodesic words that begin from basic shapes to build configurations with many more points suggests another avenue for studying equilibrium configurations both for the points on the surface of the sphere and for points on the plane, a related problem also to be examined in another paper [11].

#### Acknowledgement

This research was partially supported by grant R-151-000-015-112 at the National University of Singapore. We would like to thank the faculty and staff of

Computational Science at the NUS and the Dean of Science of the NUS for their hospitality and support of this work.

#### REFERENCES

- [1] Eric Lewin Altschuler, Timothy J. Williams, Edward R. Ratner, Robert Tipton, Richard Stong, Farid Dowla, and Frederick Wooten. *Possible Minimum Lattice Configurations for Thompson's Problem of Charges on a Sphere*. Physical Review Letters Volume 78 Number 14, (7 April 1997), 2681-2685
- [2] B. Bergersen, D. Boal, and P. Palffy-Muhoray, *Equilibrium configurations of particles on a sphere: the case of logarithmic interactions*. J. Phys. A: Math. Gen. 27 (1994) 2579-2586.
- [3] John R. Baumgardner, Paul O. Frederickson, *Icosahedron Discretization of the Two-Sphere*. SIAM Journal on Numerical Analysis 22 (December 1985), 1107-1115.
- [4] M. Bowick, A. Cacciuto, D. R. Nelson, and A. Traasset. *Crystalline Order on a Sphere and the Generalized Thompson Problem*. [http://arxiv.org/PS\\_cache/cond-mat/pdf/0206/0206144.pdf](http://arxiv.org/PS_cache/cond-mat/pdf/0206/0206144.pdf)
- [5] H. S. M. Coxeter, LL.D, FRS, *Regular Polytopes 2nd Edition*. MacMillan Company, New York, 1963.
- [6] J.P. Hansen and I.R. McDonald, *Theory of simple liquids, 2nd ed.*, Academic Press, London, 1986.
- [7] Y. Kimura and H. Okamoto, *Vortex motion on a sphere*. J. Phys. Soc. Japan **56** 1987, 4203-4206.
- [8] Chjan C. Lim, *Relative equilibria of symmetric n-body problems on the sphere: Inverse and Direct results*. Comm. Pure and Applied Math **LI** 1998, 341-371.
- [9] Chjan C. Lim, *Exact Solutions of an energy-entropy theory for the barotropic vorticity equation on a rotating sphere*. Physica A, February 2001, 131-158.
- [10] Chjan Lim, James Montaldi, Mark Roberts, *Relative Equilibria of Point Vortices on the Sphere*. Physica D 148 (2001), 97 - 135.
- [11] Chjan C. Lim, Joseph Nebus, Syed M. Assad. *A Monte Carlo Algorithm for Free and Coaxial Ring Extremal States of the Vortex N-Body Problem on a Sphere*. Submitted for publication.
- [12] Paul K. Newton, *The N-Vortex Problem: Analytical Techniques*. Springer, New York, 2001.
- [13] E. B. Saff, A. B. J. Kuijlers. *Distributing Many Points on the Sphere*. Mathematical Intelligencer, v 19, (1997), p 5 - 11
- [14] Daud Sutton, *Platonic and Archimedean Solids*, Walker and Company, New York, 2002.

Received November 2002; revised February 2003.

DEPARTMENT OF MATHEMATICAL SCIENCES, RENSSELAER POLYTECHNIC INSTITUTE  
*E-mail address:* [limc@rpi.edu](mailto:limc@rpi.edu)

DEPARTMENT OF MATHEMATICAL SCIENCES, RENSSELAER POLYTECHNIC INSTITUTE, DEPARTMENT OF COMPUTATIONAL SCIENCE, NATIONAL UNIVERSITY OF SINGAPORE

NATIONAL UNIVERSITY OF SINGAPORE.  
*E-mail address:* [nebusj@rpi.edu](mailto:nebusj@rpi.edu)